

Probing Ionization Energies for Trace Gas Identification: The Micro Photo Electron Ionization Detector (PEID)[†]

Theodor Doll ^{1,2,3,8,*}, Jonas Oberröhrman ³, Stefan Baum ³, Robert Köhler ⁴, Helmut Schütte ⁵, Stefan Gassmann ⁵, Simon Thies ⁵, Hans Baum ³, Juan J. Velasco-Velez ⁶, Victor M. Fuenzalida ⁷ and Achim W. Hassel ⁸

¹ Hannover Medical School MHH, Biomaterial Engineering, Hannover, Germany

² Fraunhofer Institute of Toxicology and Experimental Medicine ITEM, Hannover, Germany

³ DBT GmbH, Würzburg, Germany

⁴ University of Applied Sciences and Arts, Göttingen, Germany

⁵ Jade University of Applied Sciences, Wilhelmshaven, Germany

⁶ Fritz-Haber-Institute, Physical Chemistry, Faradayweg 4-6, Berlin, Germany

⁷ Universidad de Chile, Departamento de Física, Laboratorio de Superficies, Santiago, Chile

⁸ Johannes Kepler University, Inst. for Chemical Technology of Inorganic Materials, Linz, Austria

* Correspondence: doll.theodor@mh-hannover.de Tel.: +49 511 532 1530

[†] 1st International Electronic Conference on Chemical Sensors and Analytical Chemistry (CSAC2021, 07/21)

Abstract: Micro gas sensors detect the presence of substances, but can hardly identify them. We developed a novel approach of probing referenceable ionization energies. It extends the photoionization principle towards tunable energies via replacement of photons by accelerated photo electrons. The device comprises UV-LED illumination, an atmospherically stable photoelectron emission layer with a nano-vacuum electronics accelerator realized in thin film technology and charged particle measurement. A voltage variation at the accelerator provides electrons of tunable energies. We were able to prove that variable electron energies can be used for substance detection. The resulting system reaches ambient conditions operability. The actual limitations and challenges are discussed.

Keywords: Ionization energy; photo emissive materials; ambient pressure; nano vacuum electronics

Citation: Doll, T.; Oberröhrman, J.; Baum, S.; Köhler, R.; Schütte, H.; Gassmann, S.; Thies, S.; Baum, H.; Velasco-Velez, J.J.; Fuenzalida, V.M.; Hassel, A.W.; Probing Ionization Energies for Trace Gas Identification: The Micro Photo Electron Ionization Detector (PEID), *Chem. Proc.* **2021**, *3*, x. <https://doi.org/10.3390/xxxxx>

Published: date

Publisher's Note: MDPI stays neutral with regard to jurisdictional claims in published maps and institutional affiliations.



Copyright: © 2021 by the authors. Submitted for possible open access publication under the terms and conditions of the Creative Commons Attribution (CC BY) license (<http://creativecommons.org/licenses/by/4.0/>).

1. Introduction

Sensors for detecting gases are widely used in our modern societies, whether integrated in complex control systems, as the core of measuring devices or stand-alone signal transmitters. They enable us to operate production plants safely, monitor the environment reliably or drive cars with low emissions.

For signal generation, the sensor types use a variety of physical and physicochemical effects, often derived quantities, which therefore require precisely specified environmental conditions. In addition to mass spectrometry, a sensor principle that uses the ionization potentials of substances as a fundamental physical property for substance detection would be of interest. Such a hypothetical photoionization detector (PID) with tunable wavelength has been realized with 2-photon excitation in the Laser Ion Mobility Spectrometer [1]. However, the setup is not transportable.

Early on, we presented a first miniaturizable concept using photoelectrons in air. However, the materials used for emission at that time, lanthanum boride and samarium, were not atmospherically stable and required the use of a classical UV gas discharge lamp, which led to inconclusive results [2-7]. With the fundamental development of new materials [8], we can now prove long-term stable electron emission with UV-LED in air and fundamentally validate the measurement principle in a microchip arrangement working up to atmospheric conditions.

2. Theory

The basic idea of the setup as shown in figure 1 is reminiscent of the attempts of Franck and Hertz in 1913 to determine the ionization energy of gases [9]. Here it turned out that also non-ionizing energy losses resulting from interband transitions have to be taken into account and the curves of these measurements are very smeared. However, if the electron energies in this setup were sharply defined, lines would have been seen, because the vast majority of collision processes are elastic. Our basic idea was now to realize exactly this sharpness of the electron energies also at higher pressures and thus to measure above the interband energies.

Since we want to measure up to ambient pressure, we use the concepts of nano-vacuum electronics, according to which physical processes that occur on scales in the range of the mean free path [10] run quasi interaction-free in vacuum. Self-charging processes on the same scale [11] can be used to replace the otherwise necessary Wehnelt arrangements.

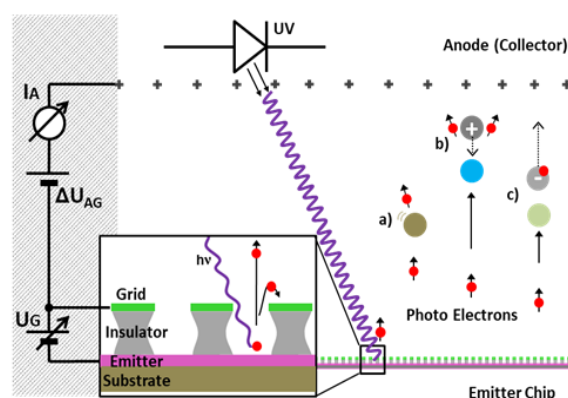


Figure 1. PEID principle: A UV LED generates photoelectrons in a nanoscale emitter, whose grid electrode accelerates the electrons to defined, variable energies. These electrons pass through the miniaturized measuring chamber and therein present trace gases. The main reactions are a) impact excitation, b) ionization with cation formation, and c) electron capture with anion formation. Electrons and anions are collected by the anode. Their current variation makes the ionization energies of the trace gases determinable if the accelerating grid voltage is properly tuned.

2.1. Electron Ionization

In Electron Ionization electrons hitting molecules generate ions. Ionization depends on the cross section for electron-molecule scattering. The cross section is characteristic for the specific ionization process and depends on the electron energy. For positive ion formation ionization starts at the ionization threshold, increasing with electron energy. In negative ion formation different processes occur that have to be included, when analyzing ionization signals. Cross section for negative ion formation is minimal at the ionization threshold energy.

2.2. Nano Vacuum Electronics

The mean free path length of electrons differs considerably from the ones for gases. First, the cross section of the electron is point-like. Secondly, the motion of the gas molecules can be disregarded, since the speed of the electrons exceeds that of the gas molecules by a thousandfold even at few eV electron energies. For an assumed particle number density of $2.7 \cdot 10^{19} \text{ cm}^{-3}$ and a diameter of the nitrogen molecules of 3.14 \AA , the mean free path of electrons at 1 bar is calculated to be 330 nm (67 % impact probability). If the dimension of the accelerating path is in this order, sharp electron energies can be expected due to predominant elastic impacts. Because of the linear dependence of the free path length on the pressure, lengths of several micrometers are obtained already at moderately reduced pressures of 100 mbar.

2.3. Photo Electron Emission

Here we estimate the expected electron current from the external photoelectric effect. Modern UV LEDs can be operated with currents in the order of 120 mA. In the short-wave UV range, their quantum yield is about 5%. Unfortunately, the external photoelectric effect has only a low electron efficiency of about 10^{-4} and corrected for the utilizable spatial angle distribution, this results in a current of generated photoelectrons of only about 20 nA. If the current losses due to the deflection of electrons to the accelerating grid are assumed to be 50%, the current available for the ionization of gas molecules is further reduced to 10 nA.

2.4. Sensitivity and Selectivity Considerations

We estimate the sensitivity of a PEID in analogy to the performance of classical PIDs. These achieve a resolution limit of 1 ppm isobutylene equivalents at a noise limit of about 1 pA of their electrometer amplifiers. The total sample volume available for ionization measurement in PID is approximately 3 mm^3 , which contains $2.7 \cdot 10^{19}$ molecules at normal pressure. At 1 ppm, in total $8 \cdot 10^{10}$ ionizable particles are contained there. If 6 million electrons per second are needed for 1 pA detection limit, these ionizable particles would be consumed in about 13,000 sec - diffusive gas exchange provides sufficient resupply here and a constant signal is obtained. This means that for classical PID an ionization probability of about 10^{-4} is sufficient. If we assume the same cross-section for electron ionization, the equivalent current change for 1 ppm detection substance in PEID would also be 1 pA, if the above calculated current of available photoelectrons were 10 nA.

Several uncertainty factors contribute to the uncertainty of the possible resolution of PEID. These are the wavelength broadening of the UV-LED in the order of 10 nm, the sharpness to which the UV-LED can be technically matched to the work function of the emitting material in the order of 30 nm, or 0.15 eV, and the more difficult to foresee effects of the boundary continuum at the work function edge of the materials, which typically cover a range of $\pm 0,12 \text{ eV}$. In sum, this corresponds to an actual uncertainty of $\pm 0.2 \text{ eV}$.

2.5. Signals Expected

The PEID resembles an electron tube (triode), which is not only operated at poor pressure [12], but with positive lattice bias U_G , which controls the electron energies. To keep the drift ratios somewhat comparable, the potential between the grid and collector anode is referenced to the grid potential with a constant, positive ΔU_{AG} . Therefore, start-up effects and the formation of space charge zones are to be expected. The expected use of gas ionization could lead to kinks in the characteristic curve, as known from e.g. tetrodes or thyratrons [13], or to fluctuations of cation space charge clouds, which could lead to visible instabilities.

Table 1. UPS data of humid air stable low work function alloys in comparison to Ag standard data.

Alloy	Intensity [cps]	Work Function [eV]	Wavelength [nm]
$\text{In}_x\text{Ce}_{(1-x)}$	$4,7 \cdot 10^5$	3,27	379
$\text{Ag}_x\text{Sm}_{(1-x)}$	$4,2 \cdot 10^5$	3,22	385
$\text{Ag}_w\text{As}_x\text{Ce}_y\text{Sm}_z$	$1,0 \cdot 10^5$	3,27	379
$\text{Ag}_x\text{Ce}_{(1-x)}$	$1,8 \cdot 10^5$	2,47	501
$\text{As}_x\text{Ce}_y\text{Sm}_z$	$1,1 \cdot 10^6$	1,87	663
Ag	n.a.	4,3	288

3. Materials and Technology

While classical PIDs work with photon energies of 10.6 eV or more, we want to avoid these direct reactions and therefore limit ourselves to energies below 5eV to also prevent

from H₂ excitation. Therefore, still without considering the availability of LEDs with these short wavelengths, many noble metals fail as emitters. The problem of base metals, however, is their oxide or hydroxide formation on the surfaces, which generally hinders the release of photoelectrons. Inspired by the unfortunately radioactive but formerly much used exception ThO₂, we have investigated compounds of noble or dignified metals with lanthanides and measured them with UPS (BESSY, Berlin) after a storage of 14 months in laboratory air. Table 1 shows that such materials can be found. For this work, we have used the materials silver and samarium-silver-cerium (see figure 2 a)

The photoemitter-accelerator device is realized in thin film technology. The electron emissive layer is sputtered on a silicon layer with a NiCr layer underneath for adhesion and atop for protection during processing. The insulator is realized in 600 nm SU8 photo resist. The accelerator grid is realized of 200 nm thin aluminum which is structured lithographically and wet etched. The resist is then etched in O₂ plasma until the emitter holes with the NiCr at the bottom is detected online. The latter is removed after chip separation and bonding using a soft 3 kV Ar ion beam.

4. Experimental Results

4.1. Measurement Setup

For the initial characterizations, the assembly of emitter accelerator chip, collector electrode and UV LED was shielded with a faraday cage and placed in a chamber allowing for variable pressures from 0.1 to 1000 mbar (figure 2b). A transimpedance amplifier, LMP 7721 (TI), was used to measure the collector current with a guard voltage follower. The UV LED (Luminus XST 3535-UV) was operated with a constant current source (figure 3i). Due to insufficient heat dissipation in the vacuum setup, its quantum efficiency was not stable due to heating, which is reflected in the following measurements.

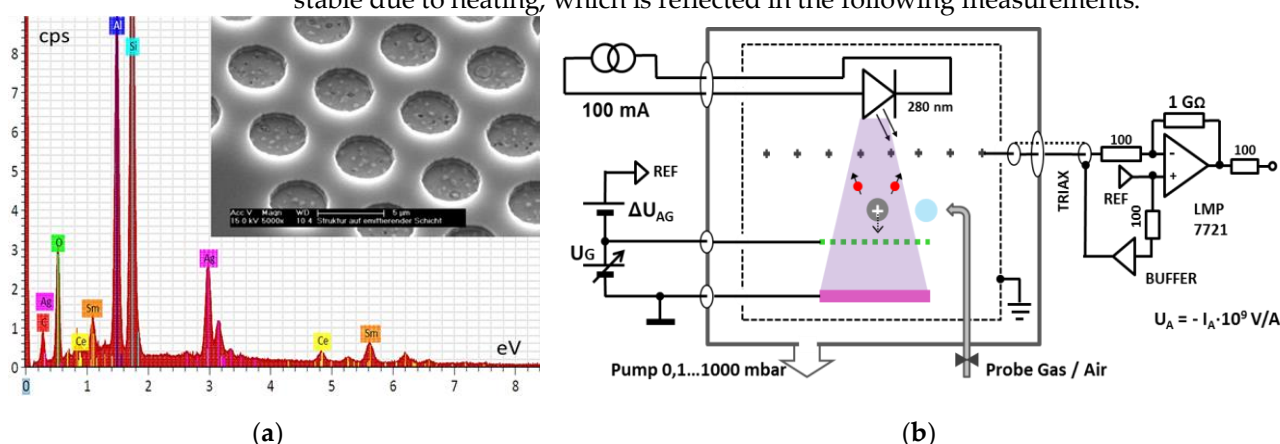


Figure 2. (a) EDX spectrum showing the composition of an AgCeSm photo emission layer at the bottom of the silicon emitter chip structure (inset, hole size: 3 μ m, accelerator grid: Al); (b) Measurement setup with electrical guarding, highly sensitive transimpedance amplifier, variable pressure pump and probe gas supply.

4.2. Device Characterization

All 8 devices under test showed a similar characteristic. True electron emission was proved and reached levels of 450 pA in fine vacuum. The devices could be operated at pressures as high as 1 bar (air), admittedly with a loss in the range of a factor of forty (figure 3ii). We further tested the energy distribution of the electrons reaching the collector electrode using the counter-field method. Here U_{Accel} is kept constant and U_A gets varied in the range $-1\text{V} < U_A < U_{\text{Accel}}$. We find that the 60% of the electrons have energies in the range $[U_{\text{Accel}}, U_{\text{Accel}}-1\text{V}]$ representing another 12% to two volts and 7% to 3 Volts below U_{Accel} .

Furthermore, we tested the possible ionization of the air components oxygen (12.06 eV) and nitrogen (15.58 eV), varying the accelerating voltages up to 20 volts under a

positive ΔU_{AG} , i.e. with all charged particles in the ionization space being detected. Here, small kinks in the current-voltage characteristic at about 14 eV appeared at times, but not reproducibly.

In a further step, we tested traces of VOCs, which we added in concentrations of the detection threshold via a wash bottle to the air flow at the throttle inlet of the vacuum reducer. At measurement pressures of about 10 mbar, there are reproducible strong fluctuations in the time course of the characteristic curve measurement, as shown in figure 3 iii for ethyl and butyl acetates (10.1 and 10.6 eV, respectively). The fluctuations occur repeatedly at voltages of 11.5 volts and above. A more precise measurement of these amplified fluctuations with fine resolution gave a limit for acetic acid (10.7 eV) of again very similar 11.6 +/- 0.2 volts (figure 3 iv).

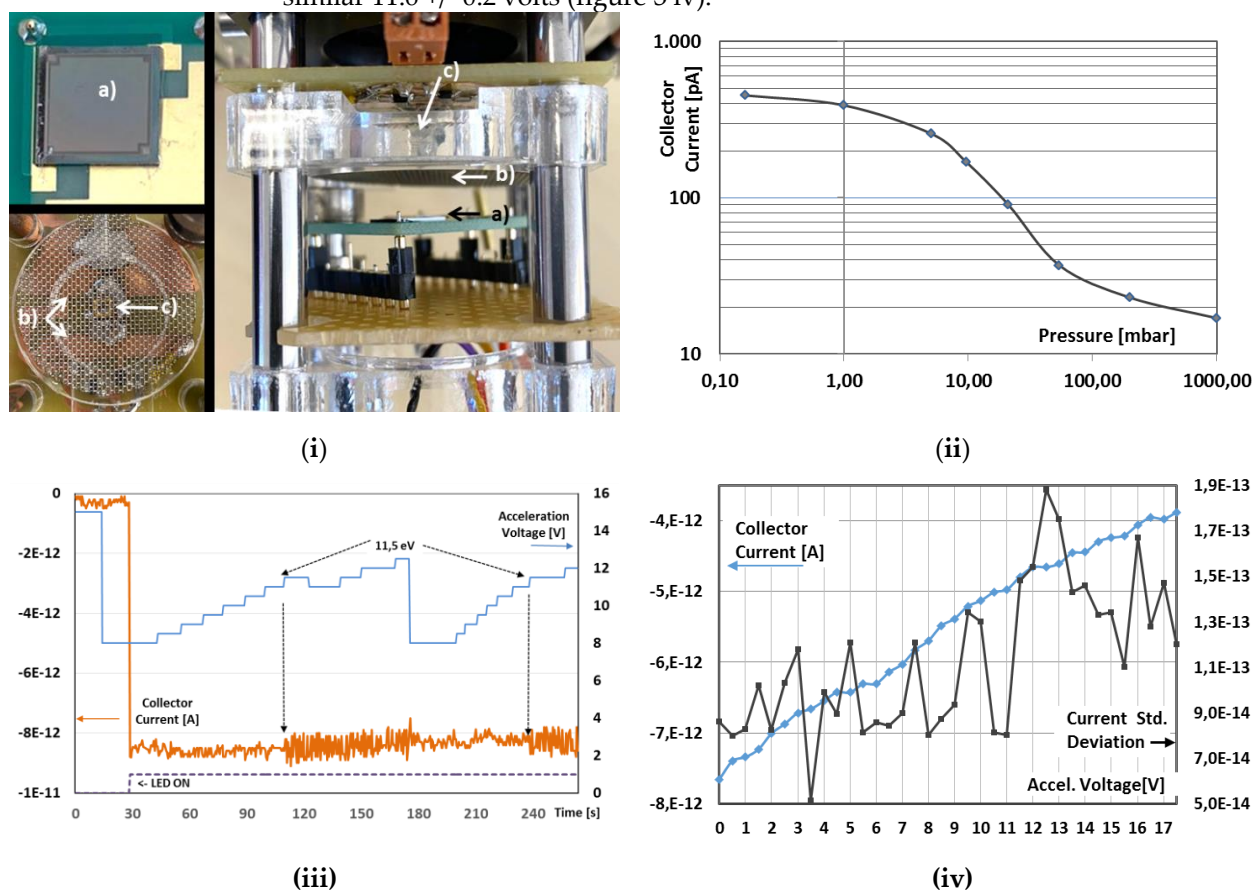


Figure 3. (i) EIPD Setup mounted on a miniature optical bench (top and side views): a):EIPD Emitter and accelerator chip on PCB sockets b) Collector Grid c) UV LED; (ii) Electron current at the collector grid at variable pressures as high as 1 bar in air; (iii) Ionization current over time with acceleration voltage variation: With ethyl and butyl acetate admixtures to air distinct and reproducible fluctuations get present from a threshold voltage; (iv) Detailed inspection of the noise fluctuations, under acetic acid in air. Almost the same threshold is obtained at 11,6 eV.

5. Discussion

We have successfully generated photoelectrons in air with new emissive materials that have proven to be atmospherically stable. These photoelectrons can be accelerated under conditions of nano-vacuum electronics and, according to the current experimental status, 60% of them still have an energy sharpness of 1 eV even at a flight and reaction length of several millimeters. A measurement procedure which keeps the electrostatic ionization conditions in the ionization space constant under varying electron energy shows that the air components O_2 and N_2 hardly interfere, although the kinks described in the literature are beginning to appear. VOC admixtures actually lead to the theoretically predicted fluctuations, possibly space charge clouds.

However, the ionization energies of the admixtures are not yet mapped with high energy. Rather, according to what has been found experimentally so far, the possibility must also be considered that in the current measurement procedure detection via an indirect O₂ ionization is seen close to the limit of 12.06 eV. This still needs to be worked on. Further measurements and deeper findings will be presented at the conference.

In general, there remain a total of 3000 potentially interesting substances whose ionization energies lie in the range of 5 - 15 eV. Within the range of the resolution accuracy theoretically estimated, we thus have 43 substances that must be considered as possible candidates for our ionization energy identification per resolution unit. This fact needs further consideration and possibly the use of prior knowledge from an AI-referenced cloud.

Author Contributions: Conceptualization, T.D. and H.B.; methodology, T.D.; software, J.O.; validation, S. B., material preparation, R.K., V.M.F and A.W.H.; material analysis, A.W.H. and J.J.V.V.; chip technology, H.S. and S.G.; resources, S.T.; data curation, J.O. and S.B.; writing T.D.; editing, R.K.; project administration, H.B.; funding acquisition, T.D. All authors have read and agreed to the published version of the manuscript.

Funding: This research was funded by the state of Bavaria (Germany) through "Bayern Innovativ" contract no.2020-5430-DB-07.

Conflicts of Interest: The authors declare no conflict of interest. The funders had no role in the design of the study; in the collection, analyses, or interpretation of data; in the writing of the manuscript, or in the decision to publish the results.

Reference

1. Oberhüttinger C., Langmeier A., Oberpriller H., Kessler M., Goebel J. and Müller G., Hydrocarbon detection using laser ion mobility spectrometry, *Int. Jour. Ion Mobility Spectr.* **2009**, 12, 23–32
2. Zimmer C., Medyanik K., Schönhense G., Krischok S., Lorenz P., Schubert J., Doll T., Low Vacuum Photo Electron Emitting Thin Films. *Phys. Status Solidi A* 1–5, **2009**, pp 484-488
3. Zimmer C. M., Schubert J., Hamann S., Kunze U., Doll T., Nanoscale photoelectron ionisation detector based on lanthanum hexaboride. *Phys. Stat. Solidi A* **2010**, DOI:10.1002/pssa.201000966(2011)
4. Haas T., Kontschew A., Zimmer C., Krage R., Doll T., Nanofunctional Electron Photo Ionization Detector, *Proc. Eurosensor XXV 2011*, Athens
5. Zimmer C., Nanostrukturierter Photoelektronenemitter auf LaB₆-Basis für atmosphärische Ionisations-Gassensorik, Dissertation Univ. Bochum, Germany, July **2011**
6. Zimmer C.M., Kallis K., Kienschik U., Schubert J., Kunze U., Doll T. "Nano photoelectron ioniser chip using LaB₆ for ambient pressure trace gas detection" *J. Microel. Eng.* 09. July **2012**
7. Kontschew A., Atmosphärische Photoionisation mit Nanometer-Samarium-Elektronemitterschichten, Dissertation Paderborn Univ., Germany, March **2013**
8. Oberroehrmann J., Hassel A., Baum H., Gaßmann S., Schütte H., Madueira M., Doll T., Photoemitting Surfaces of Low Work Function for Ionization Sensors, Proceedings Engineering of Functional Interfaces EnFI 2017, Leuven, July 8-9 **2019**
9. Franck J., Hertz G.: Über Zusammenstöße zwischen Elektronen und Molekülen des Quecksilberdampfes und die Ionisierungsspannung desselben. *Verh. D. Phys. Ges.* Vol.16, **1914**, pp. 457–467
10. Feynman R., There's Plenty of Room at the Bottom, CalTech Archives, Pasadena, 29 December **1959**
11. Doll T., Vuckovic J., Hochberg M., Scherer A., Low Energy Beam Focussing in Self-Organized Porous Alumina Vacuum Windows, *Appl. Phys. Let.* 76, 24, **2000**
12. Barkhausen H., Elektronen-Röhren Vol. 1, Hirzel, Leipzig **1928**
13. Jenkins J. and Jarvis W.H., "Basic Principles of Electronics, Volume 1 Thermionics", Pergamon Press **1966**, Ch.1.10 p.9